



Revision of the tensile database for V–Ti and V–Cr–Ti alloys tested at ANL¹

M.C. Billone^{*}, H.M. Chung, D.L. Smith

Fusion Power Program, Argonne National Laboratory, Energy Tech. and Tech. Development Divs., Argonne, IL 60439, USA

Abstract

The database for the tensile properties of unirradiated and irradiated V–(0–18) wt%Ti and V–(4–15) wt%Cr–(3–15) wt%Ti alloys tested at Argonne National Laboratory (ANL) has been reviewed and, when necessary, revised. A consistent methodology, based on ASTM terminology and standards, has been used to reanalyze the unpublished load vs. displacement curves for 162 unirradiated samples and 91 irradiated samples to determine revised values for yield strength (YS), ultimate tensile strength (UTS), uniform elongation (UE), and total elongation (TE). The revised values for UE and TE are lower by $5 \pm 2\%$ (strain) and $4 \pm 2\%$ (strain), respectively, than previously reported values, which included displacements due to machine compliance. Revised values for YS and UTS are consistent with previously published values in that they are within the scatter usually associated with these properties. © 1998 Elsevier Science B.V. All rights reserved.

1. Introduction

The results of tensile tests performed at Argonne National Laboratory (ANL) on unirradiated and irradiated V–Ti and V–Cr–Ti alloys have been reported in tabular and/or graphical form in the Fusion Reactor Materials Semiannual Progress Reports DOE/ER-0313/2 through DOE/ER-0313/20 [1–9]. Results can also be found in open-literature publications from 1988 [10] to 1996 [11], but the Progress Reports contain the most detailed set of results for the tensile properties of interest: yield strength (YS), ultimate tensile strength (UTS), uniform elongation (UE) and total elongation (TE). In this work, the original force–displacement strip chart recordings from these tests have been reanalyzed on the basis of a consistent set of terminology and methods established by ASTM [12]. The motivation for the reanalysis comes from the observation that the values reported for UE and TE appear to be inconsistent with the force–displacement diagrams.

The tensile specimens used in most ANL tensile tests were scaled down from the ASTM dog-bone example [12] to a gauge length of 7.62 mm and a cross-sectional area of $\approx 1 \text{ mm}^2$ (0.9–1.4 mm²). A uniform crosshead speed of 0.5 mm/min was used for these tests, giving an effective gauge-length strain rate of 0.11%/s. The nominal gauge length and cross-sectional area of the samples used to study the effects of oxidation on tensile properties were 19 mm and 4.5 mm². Based on crosshead speed, the gauge-length strain rate for these tests was 0.018%/s. Including the oxidation samples, 162 load–displacement curves for unirradiated vanadium alloys and 91 curves for FFTF- and HFIR-irradiated alloys were reanalyzed.

2. Methodology

The first step in analyzing a force–displacement curve is to determine a linearized slope (k) and zero-displacement point. The methodology used in the current work corresponds most closely to the tangent modulus approach described by ASTM. Because most of the load–displacement curves for vanadium alloys tested at ANL exhibited an elongated S shape during the initial rise in load, the modulus is determined by the tangent line

^{*} Corresponding author. Tel.: +1 630 2527146; fax: +1 630 2525287; e-mail: mike_billone@qmgate.anl.gov.

¹ Work supported by the Office of Fusion Energy Sciences, US Department of Energy, under Contract W-31-109-Eng-38.

coinciding with the most number of points in the elongated part of the S shape. The initial rise in load with crosshead displacement is influenced by the machine stiffness and the stiffness of the gauge length. Included in the term “machine stiffness” are all of the deformations outside the gauge length: load train, grips, pin supports, wide ends of the specimens, local deformation of the specimen at the pin supports, clearance between the hole in the specimen and the pin support, and deformation in the transition region of the specimen. Based on analyses of 162 force–displacement curves for unirradiated samples, the machine stiffness k is 1.20 ± 0.20 kN/mm, corresponding to an effective Young’s modulus E' of 82 ± 15 MPa/%, where the \pm values indicate standard deviation. Both k and E' are relatively insensitive to temperature. For irradiated samples, k is 1.76 ± 0.34 kN/mm and E' is 120 ± 28 MPa/%. This effective Young’s modulus is at least one order of magnitude less than the gauge length E for vanadium alloys [13]. The observation that k and E' increase with irradiation-induced hardening of the specimen suggests that the deformation in the non-gauge part plays a significant role in the initial rise in load with crosshead displacement.

For monotonically increasing load vs. displacement curves up to the maximum load, YS is the load (divided by the initial gauge cross-sectional area) that corresponds to an offset strain of 0.2%. The offset strain is determined by “analytically” or “graphically” unloading the specimen at a slope that corresponds to E' . The intersection of this line with the horizontal axis determines the offset strain. Some of the load–displacement curves that were analyzed exhibit discontinuous yielding which consists of a rise to a high load (upper yield point, UYP) followed by a drop in load to a minimum value (lower yield point, LYP) followed by a rise in load with displacement up to the maximum load. For these cases, the 0.2% offset stress may not be a good measure for YS. In the current work, YS is defined to be the minimum of the stress that corresponds to 0.2% offset and the stress that corresponds to LYP.

UTS is relatively straightforward to determine. For monotonically increasing load up to the maximum load, UTS is simply the maximum load divided by the initial gauge cross-sectional area. In the case of discontinuous yielding, the UYP may represent a higher load than the loads for the continuous part of the curve after discontinuous yielding. In such cases, the UYP is not to be used in determining UTS. UE is the offset strain corresponding to UTS. While UTS can be uniquely determined, more uncertainty is involved in determining UE, particularly for cases in which the maximum load is nearly constant over a strain range. Although the ASTM example implies that the midpoint of this flat region should be used to determine UE, the maximum offset strain corresponding to the maximum load is used in the current work. The maximum strain at peak load is more

characteristic of the UE of the gauge section prior to necking. TE corresponds to the offset strain at failure. The same slope used to determine YS and UE is used to determine TE.

Some of the load–displacement curves exhibit serrations, particularly in the region from peak load to failure load. For these cases, stress was determined to be: (a) the maximum stress for serrations characterized by an instantaneous drop in stress followed by a gradual rise (most common case); (b) the average stress for serrations characterized by a more sinusoidal variation with strain; and (c) the minimum stress for serrations characterized by an instantaneous rise in stress followed by a more gradual decrease.

3. Results

Fig. 1 shows an example of a force–displacement curve for a V–4Cr–4Ti (BL-47) tensile specimen irradiated at 430°C in FFTF to 27 dpa with 23 appm He and tensile-tested at 425°C. The curve shows the initial change in slope, along with the slight discontinuities with load-cell recording scale change, and the serrations in the region of the UTS. Fig. 2 shows the simplifications made in deriving the engineering stress–strain curve from the load–displacement data in Fig. 1. The

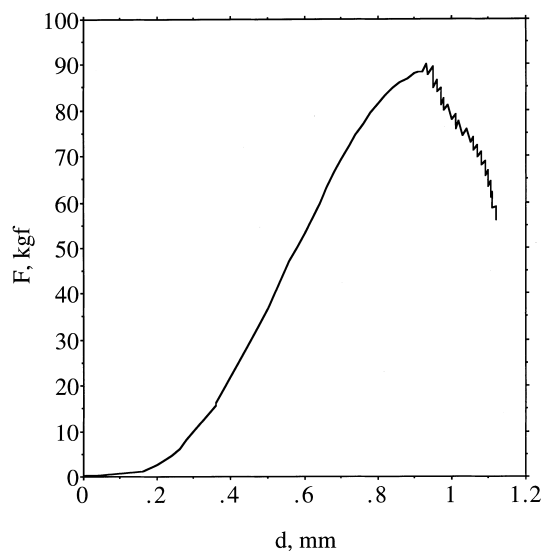


Fig. 1. Load (F)/displacement (d) curve for V–4.1Cr–4.3Ti alloy BL-47 (FFTF Cycle 12, MOTA 2B position 4D2) at 425°C after irradiation in FFTF (DHCE) at 430°C to 27 dpa with 23 appm He. Tensile specimen gauge length (L_0) and cross-sectional area (A_0) are 7.62 mm and 1.26 mm², respectively. Scale changes occurred at $d=0.36$ and 0.56 mm. Machine stiffness $k \approx 1.5$ kN/mm, crosshead speed is 0.5 mm/min and strip-chart recording speed is 50 mm/min.

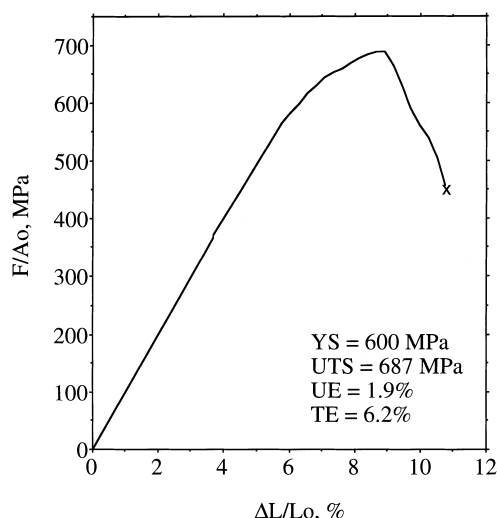


Fig. 2. Engineering stress–strain curve for V–4.1Cr–4.3Ti alloy BL-47 (FFTF Cycle 12, MOTA 2B position 4D2) at 425°C after irradiation in FFTF (DHCE) at 430°C to 27 dpa with 23 appm He. $L_0 = 7.62$ mm, $A_0 = 1.26$ mm² and strain rate is 0.11%/s.

effective elastic modulus has been used to draw the initial linear portion of the curve and the serrations have been smoothed by taking the minimum values to generate a continuous curve. The results of graphical analysis for YS, UTS, UE and TE are also presented in Fig. 2. Linearizing the initial rise in stress with strain and smoothing of the serrations were used to construct the engineering stress–strain curves for all of the cases analyzed.

Fig. 3 shows a family of stress–strain curves for a single heat (BL-47) of V–4Cr–4Ti samples irradiated in FFTF and HFIR and tested at 400–430°C, as compared to an unirradiated sample tested at 420°C. The irradiation-induced hardening and decrease in ductility (UE and TE) are apparent from these curves. The increase in strength and decrease in ductility for this alloy are less pronounced at irradiation/test temperatures of 500–520°C and 600°C. It is also apparent from Fig. 3 that proper subtraction of the “machine displacement” has a large impact on the reduction in UE and TE values reported in the current work as opposed to values reported in previous publications.

Detailed tabular and graphical results for the revised and previously reported YS, UTS, UE and TE values are presented in Ref. [14]. The results are summarized below for all alloys tested at ANL, as well as for the particular alloy class V–(4–5) wt%Cr–(4–5) wt%Ti.

The difference between revised and previously reported values for UTS of all vanadium alloys tested at ANL is insignificant for most of the cases analyzed. On an average, the new values differ by -3 ± 15 MPa ($-1 \pm 3\%$) for unirradiated alloys and -1 ± 6 MPa ($0 \pm 1\%$) for irradiated alloys. Overall, the deviation in

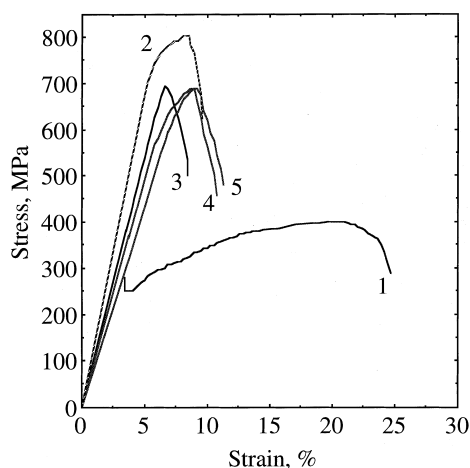


Fig. 3. Engineering stress–strain curves for unirradiated and irradiated (HFIR and FFTF Cycle 12, MOTA 2B) V–4Cr–4Ti alloy BL-47. Gauge strain rate is 0.11%/s, gauge length is 7.62 mm and cross-sectional area is 1.15–1.40 mm². Test reactor, irradiation/test temperatures, and neutron-damage-level (dpa)/He-concentration (appm) for each curve are: (1) Unirradiated, 420°C; (2) HFIR, 400/400°C, 10 dpa/ ≈ 0 appm; (3) FFTF, 427/420°C, 33 dpa/ ≈ 0 appm; (4) FFTF, 430/425°C, 27 dpa/23 appm; (5) FFTF, 430/425°C, 25 dpa/12 appm.

UTS is much less than the 10% one would expect from heat-to-heat variation for alloys of the same nominal composition. The revised values for YS differ from the previously reported values by -11 ± 19 MPa ($-4 \pm 6\%$) for unirradiated samples and 30 ± 37 MPa ($6 \pm 7\%$) for irradiated samples, well within the heat-to-heat variation in YS for structural materials. The differences between revised and previously reported values for UE and TE are more significant. All the previous values are too high because the displacement due to the non-gauge part of the samples was not properly subtracted from the crosshead displacement. The new values for UE are $-5 \pm 2\%$ (strain) lower than previously published for both unirradiated and irradiated materials. The new values for TE are $-4 \pm 2\%$ (strain) lower for both unirradiated and irradiated samples.

Because of the interest in the V–(4–5)Cr–(4–5)Ti alloys, it is worthwhile to establish baseline tensile properties for these alloys as a function of temperature. The particular compositions and heats of interest are: V–3.8Cr–3.9Ti–0.078Si (BL-71, #832665), V–4.1Cr–4.3Ti–0.087Si (BL-47, #9144), V–4.6Cr–5.1Ti–0.031Si (BL-63, #832394) and V–4.9Cr–5.1Ti–0.055Si (BL-72 or T87). Tensile samples made from these heats were machined, polished and then typically annealed at 1050–1125°C for 1 h in high quality vacuum before testing. Figs. 4 and 5 show the variations of YS and UTS and UE and TE, respectively, with temperature for unirradiated samples.

Based on the data presented in Ref. [14], V–4Cr–4Ti (heat BL-47) exhibits both an increase in strength and a

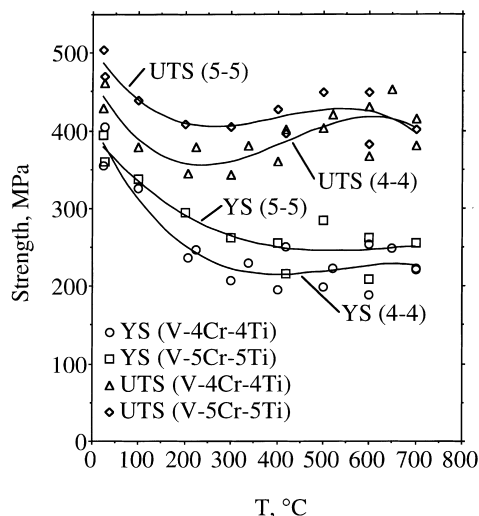


Fig. 4. Yield strength (YS) and ultimate tensile strength (UTS) vs. temperature for unirradiated V-4Cr-4Ti (BL-47 and BL-71) and V-5Cr-5Ti (BL-63 and BL-72) alloys. Solid lines represent best-fit cubic equations.

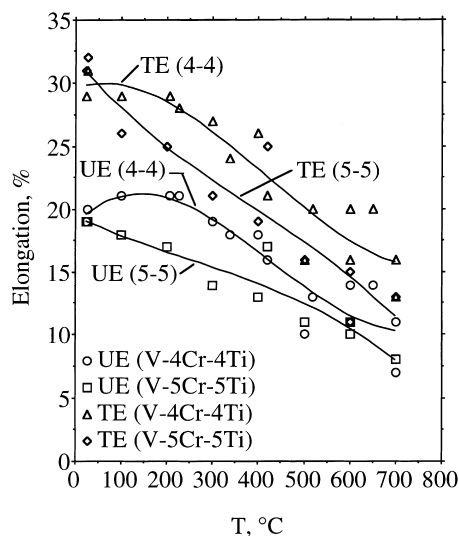


Fig. 5. Uniform (UE) and total (TE) elongation vs. temperature for unirradiated V-4Cr-4Ti (BL-47 and BL-71) and V-5Cr-5Ti (BL-63 and BL-72) alloys. Solid lines represent best-fit cubic equations.

decrease in ductility with irradiation. The degree of hardening and embrittlement decreases with the irradiation/test temperature. Using only results for samples irradiated and tested at about the same temperature, the increase in UTS is: 79% for 400–430°C, 35% for 500–520°C, and 8% for 600°C. The same pattern holds true for YS but the increases are larger: 162% for 400–430°C, 112% for 500–520°C, and 45% for 600°C. UE decreases

with irradiation to strain values of $1.6 \pm 1.0\%$ for 400–430°C, $3.6 \pm 1.3\%$ for 500–520°C and $6.5 \pm 1.1\%$ for 600°C. Similarly, TE decreases to strain values of $5.5 \pm 1.3\%$ for 400–430°C, $10 \pm 1\%$ for 500–520°C, and $13 \pm 2\%$ for 600°C.

4. Discussion

The tensile data for unirradiated and irradiated vanadium alloys tested at ANL have been reviewed and reanalyzed in accordance with ASTM procedures. The resulting values for UTS are in good agreement with values reported previously. On the average, the changes in YS values are small and well within the heat-to-heat scatter for this parameter. The differences between the new and old values for YS occur primarily due to different methodologies used in determining YS. In the current work, YS is determined to be the minimum of the 0.2% offset stress and the stress corresponding to the lower yield point. The previous YS values for unirradiated materials were mainly determined from the 0.5% offset stress criteria. For irradiated materials, several different methodologies (proportional elastic limit, upper yield point, 0.2% offset stress, etc.) were used previously. There is no single “best” way to determine YS for all structural materials and all sample sizes. The main contribution of the current set of values is that they have been determined by a consistent methodology.

The current values for UE and TE are lower than those reported previously. This arises from properly subtracting non-gauge-length deformation – included in previous values – from the total crosshead deformation. For unirradiated and irradiated alloys, the decreases in UE and TE are $5 \pm 2\%$ and $4 \pm 2\%$, respectively, where the \pm value refers to standard deviation. There is a significant impact on the ductility of the alloys irradiated and tested at 400–430°C. For unirradiated alloys and alloys irradiated/tested at $\geq 500^\circ\text{C}$, the revised values for UE are still within the ductile range (as defined by standard design codes).

The tensile data set presented in this current work should be combined with tensile data for vanadium alloys irradiated in other reactors (e.g. EBR-II, ATR, BOR-60, HFBR, etc.) at a range of temperatures and neutron damage levels to form a more complete picture of the temperatures, neutron damage levels and helium levels for which the uniform elongation decreases to a low value (e.g. $<2\%$). Currently, the number of data points for any one alloy is insufficient to determine uniform elongation transition temperatures.

The selection of V-4Cr-4Ti as a promising alloy for further development as a fusion first-wall/blanket structural material was based on engineering trade-offs between tensile strength, creep strength, ductile-to-brittle transition temperature (DBTT), tensile ductility, etc.

The laboratory heat of V–4Cr–4Ti (BL-47) exhibited low DBTT in Charpy tests, good tensile ductility, and reasonably high creep and tensile strength in the unirradiated condition. Although the tensile ductilities, UE and TE, were over-estimated in the original analysis of the data, the revised values are still high enough to justify the selection of the V–4Cr–4Ti alloy for irradiation testing. After irradiation at 400–600°C to ≤ 33 dpa, with and without He, the DBTT of BL-47 remained quite low ($\ll 0^\circ\text{C}$). It is doubtful that the revised values of UE and TE would have impacted the decision to continue R&D on V–4Cr–4Ti, as more emphasis was placed on DBTT than on UE and TE. However, the revised UE values ($1.6 \pm 1.0\%$ as compared to reported values of $\geq 8\%$) for irradiation/testing temperatures of 400–430°C may have resulted in more emphasis being placed on the planning of future irradiation tests of tensile samples in the temperature range of $400 \pm 50^\circ\text{C}$.

5. Conclusions

Review of the tensile data for V–Ti and V–Cr–Ti alloys tested at ANL indicates that there was a systematic error in the determination of UE and TE. The revised values for UE are $-5 \pm 2\%$ (strain) lower than previously reported values. The revised values for TE are $-4 \pm 2\%$ (strain) lower. Of the two, the decrease in UE is more significant, particularly for alloys irradiated/tested at 400–430°C where UE drops below 2% for some of the alloys. More tensile data on irradiated samples are needed in the temperature range of $400 \pm 50^\circ\text{C}$ and up to higher fluences and He contents to determine the temperature regime for which UE decreases to $< 2\%$ for V–Cr–Ti alloys. Other properties (e.g. fracture toughness, Charpy energy, etc.) should be obtained from samples irradiated in these temperature/fluence regimes and factored into the performance analysis to determine transition temperatures for ductile to brittle behavior of vanadium alloys. Optimization of the Cr, Ti and Si constituents, along with interstitial O, C, and N and other impurities, may be called for to achieve the best performance of vanadium alloys in terms of strength and ductility.

References

[1] B.A. Loomis, R.H. Lee, D.L. Smith, in Fusion Reactor Materials Semiannual Progress Report for Period Ending

- 31 March 1987, DOE/ER-0313/2, US Department of Energy, Office of Fusion Energy, pp. 250–258.
- [2] B.A. Loomis, R.H. Lee, D.L. Smith, in Fusion Reactor Materials Semiannual Progress Report for Period Ending 30 September 1987, DOE/ER-0313/3, US Department of Energy, Office of Fusion Energy, pp. 246–253.
- [3] B.A. Loomis, L.J. Nowicki, D.L. Smith, in Fusion Reactor Materials Semiannual Progress Report for Period Ending 31 March 1995, DOE/ER-0313/18, US Department of Energy, Office of Fusion Energy, pp. 265–272.
- [4] H.M. Chung, L. Nowicki, D. Busch, D.L. Smith, in Fusion Reactor Materials Semiannual Progress Report for Period Ending 31 December 1995, DOE/ER-0313/19, US Department of Energy, Office of Fusion Energy, pp. 17–21.
- [5] B.A. Loomis, L.J. Nowicki, D.L. Smith, in Fusion Reactor Materials Semiannual Progress Report for Period Ending 30 September 1993, DOE/ER-0313/15, US Department of Energy, Office of Fusion Energy, pp. 219–221.
- [6] H.M. Chung, B.A. Loomis, L. Nowicki, D.L. Smith, in Fusion Reactor Materials Semiannual Progress Report for Period Ending 31 December 1995, DOE/ER-0313/19, US Department of Energy, Office of Fusion Energy, pp. 77–82.
- [7] H.M. Chung, L. Nowicki, D.L. Smith, in Fusion Reactor Materials Semiannual Progress Report for Period Ending 30 June 1996, DOE/ER-0313/20, US Department of Energy, Office of Fusion Energy, pp. 78–83.
- [8] H.M. Chung, L. Nowicki, D.L. Smith, in Fusion Reactor Materials Semiannual Progress Report for Period Ending 30 June 1996, DOE/ER-0313/20, US Department of Energy, Office of Fusion Energy, pp. 84–86.
- [9] K. Natesan, W.K. Soppet, in Fusion Reactor Materials Semiannual Progress Report for Period Ending 31 December 1995, DOE/ER-0313/19, US Department of Energy, Office of Fusion Energy, pp. 50–53.
- [10] B.A. Loomis, R.H. Lee, D.L. Smith, J.R. Peterson, *J. Nucl. Mater.* 155–157 (1988) 631.
- [11] H.M. Chung, B.A. Loomis, D.L. Smith, *J. Nucl. Mater.* 233–237 (1996) 466–475.
- [12] 1996 Annual Book of ASTM Standards, Section 3: Metals Test Methods and Analytical Procedures, vol. 03.01; Metals – Mechanical Testing, Elevated and Low-Temperature Tests, Metallography, Designation E 6 (Standard Terminology Relating to Methods of Mechanical Testing, pp. 17–26) and Designation E 8 (Standard Test Methods for Tension Testing of Metallic Materials, pp. 55–96), ASTM, West Conshohocken, PA.
- [13] W.A. Simpson, in Fusion Reactor Materials Semiannual Progress Report for Period Ending 31 March 1994, DOE/ER-0313/16, US Department of Energy, Office of Fusion Energy, pp. 258–259.
- [14] M.C. Billone, in Fusion Reactor Materials Semiannual Progress Report for Period Ending 31 December 1997, DOE/ER-0313/23, US Department of Energy, Office of Fusion Energy, pp. 3–61.